Subtilisin BPN′ Variants: Increased Hydrolytic Activity on Surface-Bound Substrates via Decreased Surface Activity

Philip F. Brode III,* Christopher R. Erwin,‡ Deborah S. Rauch, Bobby L. Barnett, James M. Armpriester, Ellen S. F. Wang, and Donn N. Rubingh

Miami Valley Laboratories, The Procter & Gamble Company, Cincinnati, Ohio 45253-8707

Received August 21, 1995; Revised Manuscript Received December 18, 1995[⊗]

ABSTRACT: Site-directed mutagenesis and random mutagenesis were used to produce variants of subtilisin BPN′ (*Bacillus amyloliquefaciens*) protease with variable surface adsorption properties. Protease adsorption and peptide hydrolysis rate were measured for these variants using a model substrate consisting of a peptide covalently bound to a surface. While most variants adsorb at a level very similar to that of native BPN′, several variants were identified which adsorb either more or less. For *surface-bound* substrates we report a linear dependence between the concentration of adsorbed protease enzyme and substrate hydrolysis, similar to the linear dependence between enzyme solution concentration and hydrolysis of *soluble* substrates. On the basis of this knowledge we hypothesized that variants designed to adsorb at a higher level on a surface-bound peptide substrate would hydrolyze that surface-bound substrate faster. Contrary to our original expectations, the variants that adsorb more on the covalently bound peptide surface hydrolyze this substrate slower. In addition, variants of BPN′ which adsorb at a lower level than native BPN′ hydrolyze the surface-bound substrate faster. Enzyme adsorption and the subsequent peptide hydrolysis are altered by substituting amino acids that modify the surface charge or hydrophobicity of the native enzyme. This effect is most dramatic when the changes were made at surface-exposed sites around the binding pocket/active site of the enzyme. One mechanism that is consistent with the data is based on the relationship between the level of adsorption and the enzyme's affinity for the surface. In this mechanism weakly adsorbed enzymes are postulated to move more rapidly from site to site on the surface, thereby increasing substrate hydrolysis.

The directed modification of proteins via changes in the amino acid sequence has become commonplace with the advent of recombinant DNA technology. Although this "protein engineering" has been applied to a number of different proteins (Oxender & Fox, 1987), one of the most studied is the proteolytic enzyme subtilisin BPN′ (BPN′) from *Bacillus amyloliquefaciens*. This 275 amino acid serine protease is an enzyme that has served as a popular model system for the study of many protein properties (Wells & Estell, 1988; Bott & Betzel, 1995).

The mutagenesis studies cited above, and others like them, have shed considerable light on the molecular parameters controlling activity and stability. However, they have not addressed other issues such as how one specifies the physical parameters controlling surface-bound substrate hydrolysis, specifically protein bound to a surface. There is considerably less work addressing these types of problems, perhaps because of their greater complexity, the poor understanding of the important variables, and until recently, the lack of theoretical approaches. Gast et al. recently developed a theoretical model to fit their enzyme adsorption/diffusion/hydrolysis data on collagenase interacting with a surface-bound synthetic substrate (Gaspers et al., 1994, 1995).

The behavior of proteins at surfaces has been studied extensively (Andrade, 1985). Some of this work has used the powerful tools provided by the protein engineering approach to elucidate the relationship between structure and surface properties (Kato & Yutani, 1988; Muraki et al., 1988). A few generalizations about the behavior of proteins at surfaces can be made. First, proteins adsorb extensively and for many reasons. These include hydrophobic effects (Krebs & Phillips, 1983), electrostatic interactions (Barroug et al., 1989), and conformational changes (Kato & Yutani, 1988; Norde et al., 1986). Whether conformational changes occur upon adsorption will depend on the nature of the interface and the intrinsic stability of the protein (Norde, 1992). For enzymes, such conformational changes can result in loss of activity; however, lipolytic enzymes are a well-known example where the opposite occurs, i.e., activation of the enzyme through an interfacially induced conformational change. Examples of adsorption with loss of activity (Ghosh & Bull, 1962) and without loss of activity (McLaren & Parker, 1970) can be found in the literature. Finally, many proteins show a maximum in the amount adsorbed at the isoelectric pH (Lee & Ruckenstein, 1988; Norde, 1986), which can be attributed to the maximized conformational changes and minimized intermolecular repulsion that occur at the isoelectric point.

Not unexpectedly, the relationship between surface properties and hydrolysis has been studied most frequently for enzymes such as lipase and cellulase, which function explicitly at the interface between a surface-bound substrate (e.g., triglycerides or cellulose) and the solution containing the enzyme (Brockman, 1984; Stahlberg et al., 1991). Two

‡ Present address: Pediatric Surgery Research, Children's Hospital Research Foundation, 3333 Burnet Ave., Cincinnati, OH 45229.

⊗ Abstract published in *Advance ACS Abstracts,* February 15, 1996.

0006-2960/96/0435-3162$12.00/0

studies have been published relating the kinetics of surface hydrolysis by BPN′ to the surface properties of the enzyme (Brode & Rauch, 1992; Rubingh & Bauer, 1992). Although these studies were done on very different substrates, some common notable features were found which support the importance of the surface concentration of enzyme in controlling the rate of catalyzed hydrolysis of surface-bound substrates. In a related study, the stability of subtilisin BPN′ on hydrophilic and hydrophobic surfaces was shown to be increased by designing variants that adsorb at a lower level on these surfaces (Brode et al., 1994). Recent work on a closely related alkaline protease describes the engineering of surface charge to change adsorption properties (Egmond et al., 1994; Aehle et al., 1993).

In this study we attempt to delineate the molecular parameters that control the adsorption and hydrolytic properties of BPN′ by studying variants with modified surface interactions. Unexpectedly, enzymes which adsorb less have a greater hydrolysis rate. This suggests that, under the dilute solution conditions of these experiments, surface mobility plays a more important role than surface concentration in providing increased hydrolytic activity on surface-bound substrates.

MATERIALS AND METHODS

Enzymes

Strains, Phage, and Phagemid. The *Bacillus subtilis* protease-deficient strain BG2036 (Yang et al., 1984) and expression phagemid pSS-5 (Mitchinson & Wells, 1989) which contains the *B. amyloliquefaciens* subtilisin gene (Wells et al., 1983) were provided by Dr. J. A. Wells. For *Escherichia coli* strains, MM294 was obtained from Dr. J. A. Wells and CJ236 from Dr. T. A. Kunkel (Kunkel et al., 1987). The helper phage VCSM13 was purchased from Stratagene (La Jolla, CA).

Mutagenesis. Site-directed mutagenesis was done as previously described (Brode et al., 1994). For some of the mutants, a modified pSS-5 with a frame-shift stop codon mutation at amino acid 217 was used to produce the uracil template. Oligonucleotides were designed to restore the proper reading frame at position 217 and also encoded for random substitutions at positions 203, 213, and 217 (equimolar mixture of all four nucleotides for all three bases at these codons). Mutations that correct for the frame-shift stop and produce a functional enzyme were identified by their ability to digest casein. Random mutagenesis for the region of amino acids 200−220 was performed by spiking the nucleotides used to make oligonucleotides with 1.5%, 3.75%, or 7.5% of an equimolar mixture of the three other bases for each position (Blacklow & Knowles, 1991). These spiked oligonucleotides were then used to produce random mutant libraries from which functional enzymes were selected as above. Approximately 2000 clones were isolated and combined to make a library which was used for the adsorption screen.

Adsorption Screen for Random Variants. The random mutant library was diluted with 2×YT media so that when dispensed into 96-well microtiter plates each well would have on average a single bacterium. Each plate also included controls in the form of three wells each of similarly diluted wild-type (baseline), Y217L[1] (low adsorption control), and K213F (high adsorption control) clones, plus 15 wells started with BG2036 without the pSS-5 phagemid. The microtiter plates were incubated at 37 °C for approximately 16 h in a damp box with 225 rpm shaking. After growth the 15 wells containing bacteria without pSS-5 phagemid were spiked with varying concentrations of subtilisin BPN′ enzyme to be used as a standard curve in later steps in the process. Culture cell density was determined using a Molecular Devices V_{max} kinetics microplate reader at A_{600}. A portion of the culture was prepared for the adsorption screen by making a 1:10 dilution into an Immulon 2 plate. Glycerol was added to the culture remaining in the growth plate and stored at −70 °C. The diluted culture was filtered through a Pall (Glen Cove, NY) Loprodyne plate (low protein binding) to remove bacteria. This cleared broth was then split three ways for further analysis. One portion from each well was run through the *p*NA assay (details below) to quantitate enzyme activity. A second portion was diluted further and run through an ELISA assay (details below) to quantitate the active enzyme. The third portion was filtered through a Pall (Glen Cove, NY) Biodyne A plate and pNA assayed to quantitate the amount of enzyme activity loss due to adsorption on this Biodyne A membrane. The data were then placed in a Microsoft Excel spreadsheet to calculate the level of adsorption for each of the variants relative to the low adsorption control (Y217L), high adsorption control (K213F), and the wild-type enzyme baseline. Variants were selected that were both high and low adsorbers. Bacteria from the stored glycerol plates for the selected wells were streaked out, and an isolated clone was used to produce a new culture. From this culture the adsorption screen was repeated using eight wells for each selected variant. If the adsorption results were confirmed by this second round of selection, DNA sequencing was done to determine the mutation before fermentation, purification, and further analysis.

Fermentation and Purification. Fermentation was done using a Biostat ED fermenter (B. Braun Biotech, Inc., Allentown, PA), and purification to ≥95% activity was done as previously described (Brode et al., 1994).

Enzyme Assays. The *p*NA assay (DelMar et al., 1979) was used to determine the active enzyme concentration which is proportional to the rate of *p*-nitroaniline release from the hydrolysis reaction of the soluble synthetic substrate (Bachem, Inc., Torrance, CA) succinylalanylalanylprolylphenylalanine-*p*-nitroanilide (sAAPF-*p*NA) measured on a DU-70 spectrophotometer (Beckman Instruments, Inc.). The proportionality constants (conversion factors) used in the *p*NA assay to calculate the absolute enzyme concentrations were determined for all variants (relative to wild-type BPN′) as a part of the adsorption screen, and again more quantitatively on each selected variant via an ELISA. Finally, absorbance measurements at 280 nm were used to determine the total protein concentration ($a^{0.1\%}_{280nm} = 1.17$ for wild-type BPN′) (Matsubara et al., 1965). For the BPN′ variants, the same value for absorptivity was used unless the variant had changes involving tryptophans or tyrosines, in which case

[1] Single-letter amino acid codes are used in the following convention for naming variant enzymes: (original amino acid)(molecular position)-(new amino acid). When a variant has more than one position changed, these are combined with + signs (e.g., K213E+A216E).

the absorptivity was adjusted on the basis of the individual contribution of these amino acids. (For each tryptophan or tyrosine added/removed, the 1.17 value was adjusted up/down by 0.200 or 0.054, respectively.) The active enzyme/total protein ratio gives the enzyme percent activity.

ELISAs. In order to measure the conversion factor for the enzyme assays described above, an ELISA sandwich assay in 96-well plates was used. The ELISA plates were prepared by reacting subtilisin BPN′ antibodies (Battelle Laboratories, Columbus, OH) with the surface of the wells of Immulon 4 microtiter plates (Dynatech Laboratories, Chantilly, VA) for 18−24 h at room temperature in a damp box. After the antibody solution was suctioned out, each well was washed twice with Dulbecco's phosphate-buffered saline (PBS) (Life Technologies, Inc., Grand Island, NY). A 3% BSA (bovine serum albumin) (Sigma Chemical Co., St. Louis)/PBS solution was then equilibrated in each well for 2 h to block nonspecific binding sites. This BSA was removed by suction, and the wells were again washed twice with PBS. The plates were then dried, sealed, and stored at 4 °C until use.

All plates used in the assay had a consistent layout. Three columns of wells contained the wild-type BPN′ in known amounts for standard curve generation, and three columns contained a variant with a known conversion factor. Conversion factors for these standards had been determined previously (Brode et al., 1994) via batch and column active site titration methods. The new variants were placed in the remaining columns of the plates.

Immulon 2 plates (Dynatech Laboratories, Chantilly, VA) were used to prepare the starting solutions from the purified enzyme stocks. These plates were then appropriately diluted [with 10 mM 3-(*N*-morpholino)propanesulfonic acid (MOPS, Sigma Chemical Co.) buffer containing 0.1% Tween at pH 7.0] to the concentration required for the two assays that follow. The first assay was a *p*NA assay to determine the enzyme activity for each well, done just like the standard assay except in an Immulon 2 plate with the rates of hydrolysis measured on the microplate reader. The second was the ELISA in which aliquots from each well of the dilution plate were transferred to the Immulon 4 plate containing the antibodies plus alkaline phosphatase conjugate solution (Battelle Laboratories, Columbus, OH) and incubated at 37 °C for 2 h. The plates were rinsed, and the color development solution [alkaline phosphatase substrate kit (Bio-Rad, Richmond, CA)] was added and allowed to react at 37 °C for 30 min before the disodium EDTA stop solution was added. The plate was then read at 405 nm on the microplate reader. The ELISA OD's and *p*NA rates were transferred into a Microsoft Excel spreadsheet to calculate the specific activity and conversion factor for each new variant enzyme.

CPG:sAAPF-pNA Preparation. Aminopropyl controlled pore glass (CPG) purchased from CPG Inc. was used as a support for covalently attaching the sAAPF-*p*NA substrate. The reaction scheme and full details used in the preparation and characterization of the surface-bound substrate have been reported earlier (Brode & Rauch, 1992). The CPG surface was found to have 62 000 ± 7000 *p*NA molecules/μm^2. The surface area after reaction remains unchanged from the value of 50.0 m^2/g reported for the starting material. This suggests that the procedure used to add sAAPF-*p*NA to CPG does not damage its porous structure (mean pore diameter is 486 Å).

CPG Assay. Using CPG:sAAPF-*p*NA, adsorption of the enzyme and hydrolysis of the CPG-bound peptide can be measured in a single experiment. The enzyme solution (30 mL at 0.5 or 2.0 μg/mL) in Tris buffer [100 mM tris(hydroxymethyl)aminomethane, 10 mM $CaCl_2$, pH 8.6] was added to a 50 mL flask containing CPG:sAAPF-*p*NA, shaken for a period of 90 min at 25.0 °C, and the supernatant was aliquoted at various time intervals for analysis. On each aliquot enzyme concentration was measured and used to calculate the amount of adsorption on the CPG:sAAPF-*p*NA, and *p*NA concentration was measured to calculate the rate of hydrolysis of the surface-bound substrate by the adsorbed enzyme. Both the experimental procedure and the analysis of the adsorption and hydrolysis data have been explained earlier in full detail (Brode & Rauch, 1992). The assay was modified for one set of experiments to measure enzyme desorption. Just after the 10 min time point (post adsorption maximum), the enzyme in the flask was diluted with Tris buffer, and then aliquots were taken over the time course as usual.

Soluble Substrate Kinetic Analysis. The rate of catalyzed hydrolysis of the soluble substrate sAAPF-*p*NA was monitored by measuring the absorbance increase as a function of time at 410 nm on a DU-70 spectrophotometer. The enzyme concentration was held constant and was prepared to be in the range of 6−10 nM, while the substrate concentration was varied from 90 to 700 μM sAAPF-*p*NA for each kinetic determination. An absorbance data point was taken each second over a period of 900 s, and the data were transferred to a Lotus spreadsheet. Analysis for kinetic parameters was conducted in two ways. The first was the standard Lineweaver−Burk analysis in which the data in the initial part of the run (generally the first minute) were fit to a linear regression curve to give v_o. The v_o and s_o data were plotted in the standard inverse fashion to give K_M and k_{cat}. A second method plots all the data using a linearization of the integrated rate equation, allowing for the possibility of product inhibition (Cornish-Bowden, 1975), to obtain an s_o/v_o value for each s_o value. These data so generated were plotted as s_o/v_o vs s_o, known as the Hanes plot, and the slope and intercept were analyzed for the kinetic parameters. In principle, the slope of the linearized integrated rate expression can be analyzed for the product inhibition constant K_i. At pH 8.6, K_i appears to be approximately 10 times K_M although not accurately determined. Under such circumstances one would not expect differences in kinetic constants from the two methods, and indeed quite good agreement between the values obtained from the two analysis methods was found for all variants.

Molecular Modeling. Structures of variants were derived from the X-ray structure of subtilisin Novo, 1SBN.pdb, coordinates (Bott et al., 1988). The side-chain conformations for the mutated residues were selected from the most commonly observed values (Ponder & Richards, 1987) that did not create steric interactions with neighboring residues. Charges were assigned from CHARMm22 parameters (Momany & Rone, 1992).

GRASP (Nicholls et al., 1991) includes a Poison−Boltzman (PB) solver, which is a similar but simpler version of that used by *DelPhi* (Gilson & Honig, 1988; Nicholls & Honig, 1991). The fields calculated by it are for qualitative

Table 1: Kinetic Parameters and Adsorption/Hydrolysis Comparison for Wild-Type BPN′ and Variants[a]

	soluble substrate			surface-bound substrate	
BPN′ variants	k_{cat} (s^{-1})	K_M (10^{-4} M)	k_{cat}/K_M (10^3 s^{-1} M^{-1})	adsorption (% wild type)	hydrolysis (% wild type)
K213E+A216E	59	1.5	400	61	181
K213E+Y217L	232	3.9	599	59	178
A216E	56	1.3	425	69	165
Q206P+G211A+A216E	80	2.3	348	67	162
Y217M	128	1.9	667	67	147
Q206E	53	1.1	481	86	143
Y217L	209	3.8	550	80	141
K213E	51	1.5	340	82	124
wild-type BPN′	52	1.4	378	100	100
K213V	53	1.3	408	111	102
V203K	53	1.5	347	133	85
Q206K	46	1.0	483	124	78
K213Y	49	1.3	389	122	59
S204F+L209F	119	2.3	505	170	22

[a] Values determined as outlined under Materials and Methods.

use only. The *GRASP* PB solver uses two 33 cubed grids, one nested within the other. The inner grid dimension is set to be larger, by the diameter of one water molecule, than the maximum *x*, *y*, *z* dimension of the collection of atoms used in the calculation. The second grid is twice as large as the first, with the same center. The potentials on the outer grid are solved for first, then interpolated and refined further on the inner grid. Potentials are then interpolated to a 65 cubed grid the same size as the outer grid.

RESULTS

Michaelis−Menten Kinetic Parameters. The hydrolytic activity of enzymes is usually characterized by their ability to hydrolyze a small synthetic peptide substrate. For subtilisin BPN′ and its variants this is most frequently the soluble substrate sAAPF-*p*NA. Using the sAAPF-*p*NA substrate we measured the rate of hydrolysis for wild-type BPN′ and the variants under investigation. Each variant's specific activity was calculated using the conversion factors measured above. Michaelis−Menten kinetics were then applied to the hydrolysis rate data to calculate the kinetic parameters, k_{cat} and K_M, and the catalytic efficiency, k_{cat}/K_M (Table 1).

The catalytic rate constant k_{cat} (turnover number) for wild-type BPN′ on sAAPF-*p*NA is 52 s^{-1}, which is in good agreement with the data of Wells et al. (1987). This value is not greatly changed by most of the single-site mutations introduced into the native structure, so that the k_{cat} values fall in the 52 ± 6 s^{-1} range. One notable exception to this involves variants at the 217 position in the molecule. Y217M, Y217L, and the double variant K213E+Y217L all show a significant increase in substrate turnover number. S204F+L209F is the other variant displaying a k_{cat} that is higher than the wild-type value. Also, most of the variants bind the soluble substrate with a characteristic binding constant (K_M) in the range of 0.14 ± 0.05 mM, about the same as wild-type BPN′. Y217M is at the upper end of this range. The two Y217L variants, Q206P+G211A+A216E, and S204F+L209F are clearly different, displaying a weaker binding to the soluble substrate. As will be seen below, the ability of an enzyme to hydrolyze surface-bound peptide cannot be predicted by either k_{cat}, the soluble substrate hydrolysis rate constant, or K_M, the substrate binding constant.

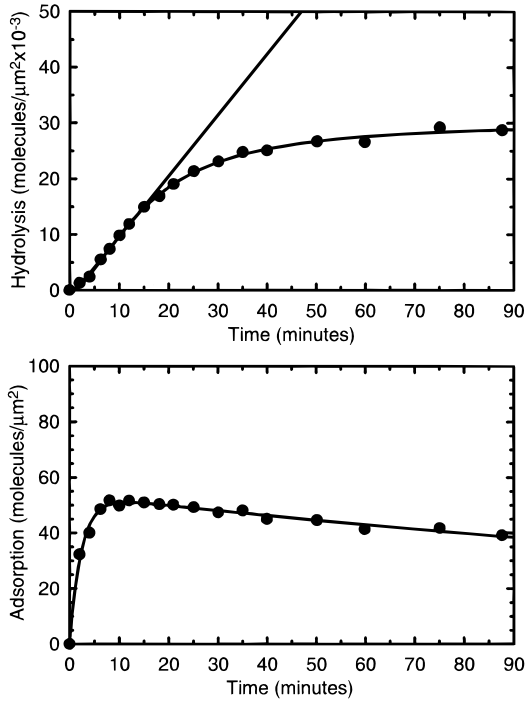

FIGURE 1: Subtilisin BPN′ variant (K213V at 0.5 μg/mL) hydrolysis of (top panel) and adsorption on (bottom panel) 0.1 g of surface-bound peptide substrate CPG:sAAPF-*p*NA.

Time Course of Adsorption and Hydrolysis of BPN′ Variants. Perhaps more pertinent to the hydrolysis of surface-bound peptide are the surface properties of the enzyme. The most directly measurable surface property is adsorption, and the technique described in Materials and Methods allows adsorption to be measured simultaneously with hydrolysis of the surface-bound peptide. The details of the technique were presented earlier along with initial results on wild-type BPN′ and the variant Y217L (Brode & Rauch, 1992). Briefly, we reported that a direct relationship between enzyme adsorbing on the peptide surface and the rate of hydrolysis of the surface-bound peptide is observed. When a lag is observed in the adsorption of the enzyme, a corresponding lag is seen for the onset of hydrolysis of the peptide from the surface. We find a very similar time-dependent behavior for variants of BPN′. Figure 1 shows this relationship between adsorption (bottom graph) and hydrolysis (top graph) for K213V. The K213V variant is

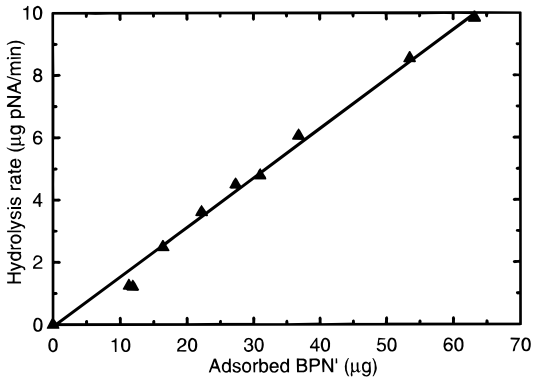

FIGURE 2: Rate of hydrolysis of surface-bound peptide substrate (CPG:sAAPF-*p*NA) as a function of amount of adsorbed wild-type BPN′.

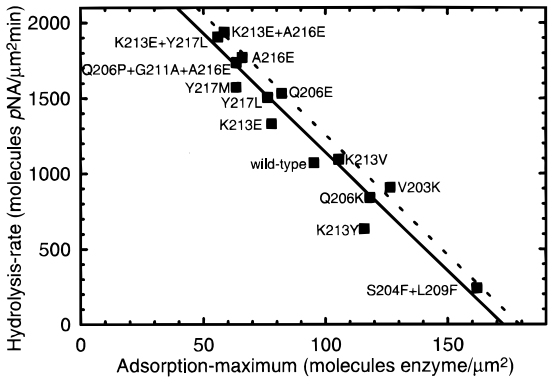

FIGURE 3: Rate of hydrolysis of surface-bound substrate (CPG: sAAPF-*p*NA) by variants of subtilisin BPN′ as a function of their level of adsorption on CPG:sAAPF-*p*NA (shown as filled squares) with linear regression (solid line). The dotted line is the linear regression through the data corrected for the concurrent desorption that occurs during the experiment and shows that the adsorption/hydrolysis correlation is unaffected by the desorption.

one of the many BPN′ variants which produces no significant change in the adsorption rate, adsorption maximum, or hydrolysis rate from the wild-type BPN′ (Brode & Rauch, 1992).

In addition, experiments in which CPG:sAAPF-*p*NA was fixed while varying the amount of enzyme show a linear relationship between the amount of enzyme adsorbed and the rate of peptide hydrolysis (Figure 2). This is consistent with results from a similar study of hydrolysis of an insoluble substrate (Azocoll) by adsorbed enzyme (Rubingh & Bauer, 1992) showing a more rapid rate of hydrolysis when more enzyme is adsorbed.

BPN′ Variants with Altered Surface Adsorption and Hydrolysis. Site-directed variants of BPN′ were made at positions all around the surface of the molecule. The vast majority provided no change in the adsorption and hydrolysis properties from the wild-type BPN′ (e.g., K213V, Figure 1) when compared at equal initial enzyme concentration. A few of the site-directed variants, however, did produce differences in these properties. The first ones identified were K213F, V203K, Q206K, and Y217L. These variants are not only at positions close in sequence but are also on a surface loop of the molecule from 200−220. This loop is on the face of the molecule in the region of the binding pocket and close to the active site triad (D32, H64, S221).

With this discovery a random library of variants from this region of the molecule was produced and screened via the adsorption screen. The screen selected BPN′ variants having surface activity that differs from wild type as measured by their relative adsorption to the Biodyne A membrane (consisting of nylon 66 with a surface chemistry that is 50% amine and 50% carboxyl groups, p*I* 6.5). We then investigated the adsorption and hydrolysis properties of many of these variants using the CPG:sAAPF-*p*NA assay. Figure 3 shows a plot of hydrolysis rate vs enzyme adsorption maximum on CPG:sAAPF-*p*NA for wild-type BPN′ and these variants, compared at equal initial enzyme concentrations. The hydrolysis rate is defined as the slope of the linear portion of the hydrolysis vs time plot (Figure 1) and is expressed as molecules of *p*NA released into solution per μm^2 per minute. The adsorption maximum is defined as the maximum level of adsorption achieved on the adsorption vs time plot (Figure 1) and is expressed as molecules of enzyme per μm^2. (After adsorption reaches a maximum it does not plateau but instead decreases as a function of time. This is the result of the surface changing as peptide hydrolysis continues. The active enzyme desorbs from the hydrolyzed surface. For this reason it could be argued that the measured maximum is not the true maximum because of the simultaneously occurring desorption. This issue was addressed by estimating an upper limit for adsorption. Calculating the rate of desorption observed immediately after the adsorption maximum, and extrapolating that rate to time 0, provides a reasonable measure of an adsorption upper limit. The dotted line in Figure 3 shows the linear fit to the adsorption determined in this way. This correction to the adsorption maximum determination does not change the variants' adsorption maximum/hydrolysis rate correlation.)

As stated, most of the site-directed variants show no change from wild-type BPN′ in their surface adsorption maximum or hydrolysis rate (e.g., K213V) and if added to Figure 3 would cluster near the wild-type BPN′ data point. However, variants identified by the adsorption screen as high adsorbers consistently adsorb significantly more on the CPG:sAAPF-*p*NA surface when compared to wild-type BPN′. The variants which adsorb more than wild type on the peptide-covered surface hydrolyze that peptide slower. The kinetic parameters listed in Table 1 for these same variants show that, on the soluble form of this substrate, sAAPF-*p*NA, their hydrolytic activities are either unchanged or in the case of S204F+L209F display higher catalytic efficiencies than wild type.

Other variants identified by the adsorption screen as low adsorbers are also found to adsorb less than wild type on the CPG:sAAPF-*p*NA and are shown in Figure 3. Consistently, the variants which adsorb less than wild type hydrolyze the peptide on the surface at a faster rate. In the case of Y217L, the increased hydrolytic activity against the soluble form of the substrate is also displayed on this surface-bound CPG:sAAPF-*p*NA. However, several variants (e.g., K213E, A216E, and K213E+A216E) having soluble kinetics that are very similar to wild type provide an increase (24%, 65%, and 81%, respectively) in hydrolysis rate over wild type on the surface-bound substrate.

Since adsorption is reversible in this system, a desorption experiment as described in Materials and Methods was done on a representative high adsorber (S204F+L209F), low adsorber (K213E+Y217L), and wild-type BPN′ to provide additional insight into the relative affinity of these variants for the model surface. After the adsorption maximum was

reached, the bulk solution was diluted by one-third and the level of adsorption measured upon reequilibration. For the high adsorber, only 4% of the adsorbed enzyme (measured as percent of adsorption maximum) desorbed back into the diluted bulk solution, while 28% of the wild type desorbed, and 45% of the low adsorber desorbed.

Molecular Modeling of Electrostatic Surface Potentials. Many of the variants which adsorb less and hydrolyze the surface-bound substrate faster than wild type contain glutamic acids (negatively charged, pK_a = 4.6) as the substituting amino acids. The variant found to adsorb the most and hydrolyze the surface-bound substrate the slowest contains (hydrophobic) phenylalanines. In order to investigate how these very different sets of substitutions affect the surface potential of the enzyme, molecular modeling was done on several variants and wild type. Figure 4 shows a comparison of the potential maps for wild type and two variants. The red coloration on the surface indicates regions of negative charge while the blue codes for positive charge. Figure 4a shows wild type for baseline comparison. Figure 4b is the representation for the low adsorber, K213E+A216E. The dramatic increase in negative surface charge can be seen in the loop region while the rest of the surface of the molecule is unchanged. Figure 4c shows that the loop surface charge for the S204F+L209F variant is only very slightly different from that of wild type.

DISCUSSION

We have compared substrate hydrolysis under two conditions. In one case the substrate is free to diffuse in solution, and in the second case it is attached to a surface. By investigating enzyme-catalyzed hydrolysis of both soluble and surface-bound substrate, we sought to answer two basic questions. First, does having the substrate in close proximity to a surface affect reaction rate? For BPN′, we have shown that the surface does have an important effect on reaction rate. In earlier work on the surface-bound substrate, we reported that the V_{max}, obtained by extrapolating the rate for the wild-type enzyme to infinite substrate concentration, was 50-fold less than the V_{max} for the soluble substrate (Brode & Rauch, 1992). This present study further supports the contention that the surface is important, showing that adsorption and catalytic activity are clearly correlated for different variants of the wild-type enzyme (Figure 3). Having established this correlation, we asked the second more complex question of what controls the rate of reaction when the substrate is surface bound?

Accepted theory for catalysis of soluble substrates is that enzymes accelerate the rate of a chemical reaction by lowering the energy barrier (activation energy) between reactants and products. For proteases catalyzing the hydrolysis of an amide bond, the transition state has been shown to be a tetrahedral intermediate, and the developing negative charge is stabilized by the oxyanion hole (nitrogen side chain of Asn155 and backbone nitrogen of Ser221). The observed decrease in catalytic effectiveness when the substrate is attached to a solid surface could occur for a number of reasons. (1) Proximity to a surface could affect the enzyme conformation, making the binding between enzyme and transition state less favorable and thereby reducing transition-state stabilization. (2) Local environmental variables such as pH, dielectric constant, and enzyme and substrate con-

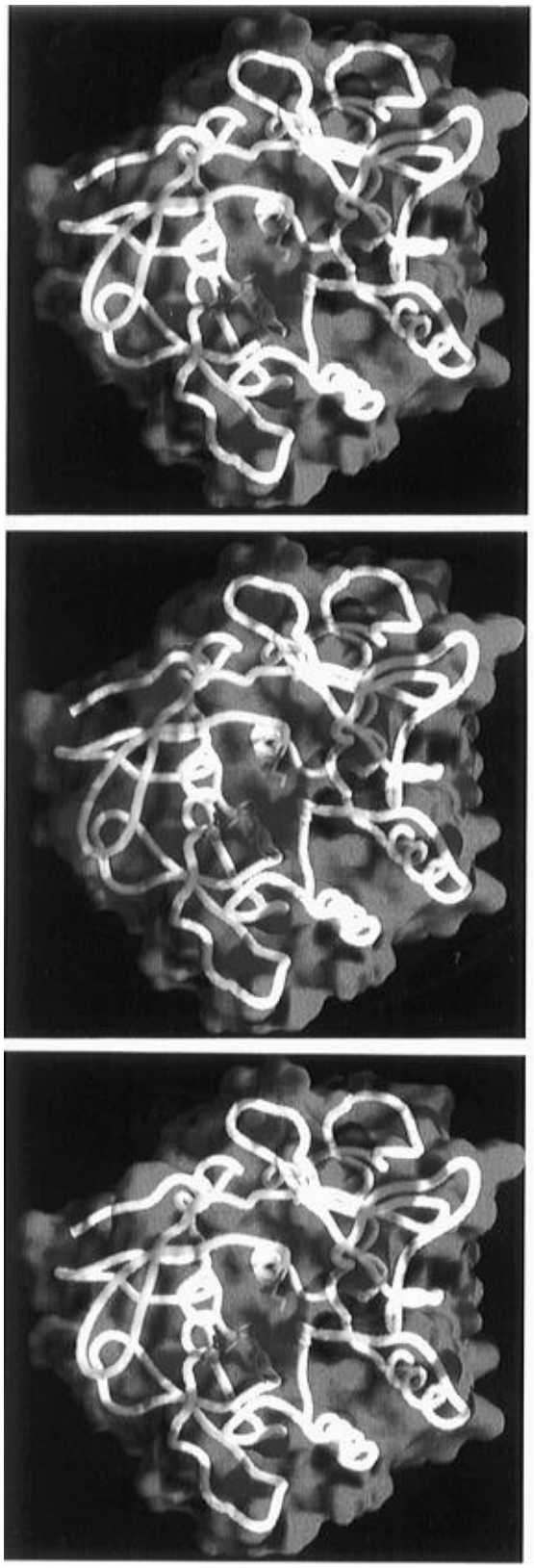

FIGURE 4: Surface potential maps for wild-type BPN′ (a, top), K213E+A216E (b, middle), and S204F+L209F (c, bottom), each showing the active site triad: serine 221 (green), histidine 64 (blue), aspartic acid 32 (red), and the 200−220 loop containing the amino acid sequence changes (yellow). Variants show altered surface potential only in the region of this loop. Red shading represents regions of negative charge, and blue shading represents positively charged regions. K213E+A216E increases the negative charge in this region relative to wild-type BPN′, while S204F+L209F causes very little change in surface potential.

centration are known to be different at the surface and could change the reaction rate. (3) Enzyme orientation may be affected as it approaches the surface. (4) The rate-limiting step in the catalytic process may be different when the substate is bound to a surface. Our data show that the rate-limiting step for the catalytic processing of surface-bound substrate is different and more specifically that the slowest step is surface mobility of the enzyme as opposed to hydrolysis rate.

The existence of a different rate limiting step for surface-bound substrate is confirmed by the fact that the double phenylalanine variant has a high k_{cat} value (for soluble substrate) but hydrolyzes surface-bound substrates poorly. In light of the observed relationship between adsorption and hydrolysis, we suggest that enzyme movement from one substrate site on the surface to another contributes, at least in part, to the observed decrease in rate. In this surface mobility mechanism the rate of enzyme movement is controlled by the energy of adsorption/desorption and the energetics of lateral diffusion across the surface. We note that Gaspers et al. (1994, 1995) have shown that mobility is related to chemical reactivity in the case of collagenase-catalyzed hydrolysis of a model peptide on a quartz slide. In this study they measured both surface diffusion and rates of reaction, concluding that the time scale of surface diffusion and the kinetics of the bond-breaking events were of similar magnitude. Accordingly, the overall reaction rate in the collagenase system is determined by both reaction and diffusion.

But how does the enzyme's surface mobility, and its hydrolysis of the surface-bound substrate, relate to the enzyme adsorption that we measured in these experiments? The presence of the surface increases the local concentration of the enzyme by adsorption. In this and earlier work (Rubingh & Bauer, 1992) we have shown that, in fact, for surface-bound substrates the rate of hydrolysis is linearly proportional to the enzyme surface concentration (Figure 2): just as when the substrate is in solution the hydrolysis rate responds linearly to the enzyme solution concentration. Having established this proportionality between adsorption and hydrolysis for BPN′ enzymes on a surface-bound substrate, it is surprising that when variants are compared at equal initial solution concentrations, those which adsorb the most hydrolyze the substrate at the slowest rate, while those which adsorb the least hydrolyze fastest. To explain this we note that the adsorption measurements are at bulk equilibrium concentrations below 2 μg/mL (70 nM). At this low concentration the adsorbed molecules sparsely populate the surface [for wild-type BPN′ $\leq$100 molecules/μm^2 or $<$0.2% of a close-packed monolayer (Brode et al., 1994)] and the adsorption is controlled by adsorbate/adsorbent forces. At these low concentrations the enzyme affinity and amount adsorbed are proportional. Thus, a variant which is adsorbed more is also more strongly adsorbed and is less mobile at the surface. Likewise, low adsorption at these low concentrations is indicative of a low-affinity (high mobility) enzyme which can hydrolyze the surface-bound peptide faster. Additional support for this relationship between adsorption and affinity is offered by the desorption data. Much less, only 4%, of the variant displaying high adsorption was desorbed upon dilution, indicating higher affinity for the surface than wild type where 28% desorbed. The surface affinity is lower in the case of the low-adsorbing variant where 45% of the adsorbed enzyme desorbed. Knowing that, for any one enzyme, higher adsorption produces a greater hydrolysis rate (Figure 2) suggests that when several different enzymes are compared, enzyme mobility is more important than absolute surface concentration in determining the hydrolysis rate.

Further support for the mobility mechanism comes from computer modeling to compare the surface potential of wild-type BPN′ with the surface potentials of variants showing altered adsorption. The variants which alter adsorption are the result of amino acid changes in a loop (amino acids 200−220) near the active site that would be expected to reside close to the surface when the substrate peptide sessile bond is in position to be cleaved by the active site serine of the enzyme. Since adsorption is affected by not only enzyme charge but also surface charge, it is essential to note that ζ potential measurements of glass surfaces show that they are negatively charged. Covalent coupling with substrate reduces but does not eliminate the charged groups (Brode et al., 1994). Enzyme mutations which increase the negative field on the surface loop (e.g., Figure 4b) are found to adsorb less on these glass surfaces, as would be expected for superposition of fields of similar charge. Conversely, mutations which create a positive charge adsorb more on the negatively charged surface. The double phenylalanine variant demonstrates that electrostatics are not the only way that adsorption can be controlled. Here we find much greater adsorption despite the fact that no charge is introduced (Figure 4c). It would appear that the hydrophobic effect is also capable of promoting adsorption and affinity to the surface.

The relative contribution of mobility and reaction to the overall rate of hydrolysis can be estimated by examining Table 1. Comparing the first two entries, K213E+A216E vs K213E+Y217L, we find that the hydrolysis rates against soluble substrate are widely different but the adsorption levels are nearly the same. These variants have hydrolysis rates for surface-bound substrate that are nearly the same as well, suggesting that adsorption (and the subsequent mobility) is more important. As a second comparison we examine Q206E and Q206K. Here the adsorption levels are widely different, but the rates of solution hydrolysis are nearly equal. The rates of hydrolysis of the surface-bound substrate also differ widely, again in good correlation with the adsorption. This correlation is strong support for enzyme surface mobility serving as the rate-limiting process. Furthermore, the introduction of a negative or positive charge in this comparison would be expected to enhance or retard, respectively, the mobility of the enzyme in the surface's negative field, and this is reflected in the rates. From these considerations we would conclude that surface diffusion is much more important than the kinetics of bond breaking for these enzymes when catalyzing the hydrolysis of surface-bound substrates.

ACKNOWLEDGMENT

We acknowledge the following people for their contributions to this research: Dan Toerner and Debbie Lade for the synthesis of oligos and for automated sequencing, Yiping Sun and Mark Bauer for mass measurements on the variants (mass spectroscopy) as an independent identity check, and Phillip Green and Debbie Thaman for assistance in the areas of protein fermentation and purification.

REFERENCES

Aehle, W., Sobek, H., Amory, A., Vetter, R., Wilke, D., & Schomburg, D. (1993) *J. Biotechnol. 28*, 31−40.

Andrade, J. D., Ed. (1985) *Surface and Interfacial Aspects of Biomedical Polymers: Volume 2 Protein Adsorption*, Plenum Press, New York.

Barroug, A., Lemaitre, J., & Rouxhet, P. G. (1989) *Colloids Surf. 37*, 339−355.

Blacklow, S. C., & Knowles, J. R. (1991) in *Directed Mutagenesis—A Practical Approach* (McPherson, M. J., Ed.) pp 177−198, IRL Press, Oxford.

Bott, R., & Betzel, C., Eds. (1995) *Advances in Experimental Medicine and Biology: Subtilisin Enzymes*, Vol. 379, Plenum Press, New York.

Bott, R., Ultsch, M., Kossiakoff, A., Graycar, T., Katz, B., & Power, S. (1988) *J. Biol. Chem. 263*, 7895−7906.

Brockman, H. L. (1984) in *Lipases* (Borgstrom, B., & Brockman, H. L., Eds.) pp 3−46, Elsevier, Amsterdam.

Brode, P. F., III, & Rauch, D. S. (1992) *Langmuir 8*, 1325−1329.

Brode, P. F., III, Erwin, C. R., Rauch, D. S., Lucas, D. S., & Rubingh, D. N. (1994) *J. Biol. Chem. 269*, 23538−23543.

Cornish-Bowden, A. (1975) *Principles of Enzyme Kinetics*, pp 142−197, Butterworths, London.

DelMar, E. G., Largman, C., Brodrick, J. W., & Geokas, M. C. (1979) *Anal. Biochem. 99*, 316−320.

Egmond, M. R., Antheunisse, W. P., van Bemmel, C. J., Ravestein, P., de Vlieg, J., Peters, H., & Branner, S. (1994) *Protein Eng. 7*, 793−800.

Gaspers, P. B., Robertson, C. R., & Gast, A. P. (1994) *Langmuir 10*, 2699−2704.

Gaspers, P. B., Gast, A. P., & Robertson, C. R. (1995) *J. Colloid Interface Sci. 172*, 518−529.

Ghosh, S., & Bull, H. B. (1962) *Arch. Biochem. Biophys. 99*, 121−125.

Gilson, M. K., & Honig, B. H. (1988) *Proteins 3*, 32−52.

Kato, A., & Yutani, K. (1988) *Protein Eng. 2*, 153−156.

Krebs, K. E., & Phillips, M. C. (1983) *Biochim. Biophys. Acta 754*, 227−230.

Kunkel, T. A., Roberts, J. D., & Zakour, R. A. (1987) *Methods Enzymol. 154*, 367−382.

Lee, S. H., & Ruckenstein, E. (1988) *J. Colloid Interface Sci. 125*, 365−379.

Matsubara, H., Kasper, C. B., Brown, D. M., & Smith, E. L. (1965) *J. Biol. Chem. 240*, 1125−1130.

McLaren, A. D., & Packer, L. A. (1970) *Adv. Enzymol. 33*, 245−308.

Mitchinson, C., & Wells, J. A. (1989) *Biochemistry 28*, 4807−4815.

Momany, F. A., & Rone, R. (1992) *J. Comput. Chem. 13*, 888−900.

Muraki, M., Morikawa, M., Jigami, Y., & Tanaka, H. (1988) *Protein Eng. 2*, 49−54.

Nicholls, A., & Honig, B. (1991) *J. Comput. Chem. 12*, 435−445.

Nicholls, A., Sharp, K. A., & Honig, B. (1991) *Proteins 11*, 281−296.

Norde, W. (1986) *Adv. Colloid Interface Sci. 25*, 267−340.

Norde, W. (1992) *J. Dispersion Sci. Technol. 13*, 363−367.

Norde, W., MacRitchie, F., Nowicka, G., & Lyklema, J. (1986) *J. Colloid Interface Sci. 112*, 447−456.

Oxender, D. L., & Fox C. F., Eds. (1987) *Protein Engineering*, Alan R. Liss Inc., New York.

Ponder, J. W., & Richards, F. M. (1987) *J. Mol. Biol. 193*, 775−791.

Rubingh, D. N., & Bauer, M. D. (1992) in *Polymer Solutions, Blends and Interfaces* (Noda, I., & Rubingh, D. N., Eds.) pp 445−464, Elsevier, Amsterdam.

Stahlberg, J., Johansson, G., & Pettersson, G. (1991) *Biotechnology 9*, 286−290.

Wells, J. A., & Estell, D. A. (1988) *Trends Biochem. Sci. 13*, 291−297.

Wells, J. A., Ferrari, E., Henner, D. J., Estell, D. A., & Chen, E. Y. (1983) *Nucleic Acids Res. 11*, 7911−7925.

Wells, J. A., Cunningham, B. C., Graycar, T. P., & Estell, D. A. (1987) *Proc. Natl. Acad. Sci. U.S.A. 84*, 5167−5171.

Yang, M. Y., Ferrari, E., & Henner, D. J. (1984) *J. Bacteriol. 160*, 15−21.

BI951990H